

**NASA
Reference
Publication
1123**

July 1984

Design of Power- Transmitting Shafts

Stuart H. Loewenthal

NASA

1
2
3
4
5
6
7
8
9
10
11
12
13
14
15
16
17
18
19
20
21
22
23
24
25
26
27
28
29
30
31
32
33
34
35
36
37
38
39
40
41
42
43
44
45
46
47
48
49
50
51
52
53
54
55
56
57
58
59
60
61
62
63
64
65
66
67
68
69
70
71
72
73
74
75
76
77
78
79
80
81
82
83
84
85
86
87
88
89
90
91
92
93
94
95
96
97
98
99
100

NASA
Reference
Publication
1123

1984

Design of Power- Transmitting Shafts

Stuart H. Loewenthal

Lewis Research Center
Cleveland, Ohio

NASA

National Aeronautics
and Space Administration

Scientific and Technical
Information Branch

Contents

Summary.....	1
Introduction.....	1
Symbols	1
Static or Steady Loading	2
Pure Torque	2
Simple Bending	3
Combined Torsion, Bending, and Axial Loading	3
Fluctuating Loads.....	6
Simple Loading	7
Fluctuating Bending	8
Fluctuating Torsion	8
Fatigue Under Combined Stresses	8
Reversed Bending with Steady Torsion	9
Fluctuating Bending Combined with Fluctuating Torsion.....	9
Fatigue Life Modifying Factors.....	9
Surface Factor k_a	9
Size Factor k_b	10
Reliability Factor k_c	11
Temperature Factor k_d	12
Fatigue Stress Concentration Factor k_e	12
Press-Fitted Collar Factor k_f	13
Residual Stress Factor k_g	13
Corrosion Fatigue Factor k_h	15
Miscellaneous Effects Factor k_i	15
Variable-Amplitude Loading.....	15
Short-Life Design.....	16
Intermediate- and Long-Life Design	16
Application Example	18
Rigidity.....	19
Shaft Materials	20
Shaft Vibration.....	21
References	22

Summary

Power transmission shafting is a vital element of all rotating machinery. This report summarizes design methods, based on strength considerations, for sizing shafts and axles to withstand both steady and fluctuating loads. The effects of combined bending, torsional, and axial loads are considered along with many application factors that are known to influence the fatigue strength of shafting materials. Methods are presented to account for variable-amplitude loading histories and their influence on limited-life designs. The influences of shaft rigidity, materials, and vibration on the design are also discussed.

Introduction

The term "shaft" applies to rotating machine members used for transmitting power or torque. The shaft is subject to torsion, bending, and occasionally axial loading. Stationary and rotating members, called axles, carry rotating elements, and are subjected primarily to bending. Transmission or line shafts are relatively long shafts that transmit torque from motor to machine. Countershafts are short shafts between the driver motor and the driven machine. Head shafts or stub shafts are shafts directly connected to the motor.

Motion or power can be transmitted through an angle without gear trains, chains, or belts by using flexible shafting. Such shafting is fabricated by building up on a single central wire one or more superimposed layers of coiled wire (ref. 1).

Regardless of design requirements, care must be taken to reduce the stress concentration in notches, keyways, etc. Proper consideration of notch sensitivity can improve the strength more significantly than material consideration. Equally important to the design is the proper consideration of factors known to influence the fatigue strength of the shaft, such as surface condition, size, temperature, residual stress, and corrosive environment.

High-speed shafts require not only higher shaft stiffness but also stiff bearing supports, machine housings, etc. High-speed shafts must be carefully checked for static and dynamic unbalance and for first- and second-order critical speeds. The design of shafts in some cases,

such as those for turbopumps, is dictated by shaft dynamics rather than by fatigue strength considerations (ref. 2).

The lengths of journals, clutches, pulleys, and hubs should be viewed critically because they very strongly influence the overall assembly length. Pulleys, gear couplings, etc., should be placed as close as possible to the bearing supports in order to reduce the bending stresses.

The dimensions of shafts designed for fatigue or static strength are selected relative to the working stress of the shaft material, the torque, the bending loads to be sustained, and any stress concentrations or other factors influencing fatigue strength. Shafts designed for rigidity have one or more dimensions exceeding those determined by strength criteria in order to meet deflection requirements on axial twist, lateral deflection, or some combination thereof. An increase in shaft diameter may also be required to avoid unwanted critical speeds.

Symbols

A	shaft cross-sectional area, m^2 (in^2)
B	hollowness factor
b	slope of stress-life curve on log-log coordinates or fatigue strength exponent (taken as positive value)
D	shaft diameter, defined in figs. 1 and 2, mm (in.)
d	shaft diameter, defined in fig. 1, mm (in.)
d_i	inside diameter, mm (in.)
d_o	outside diameter, mm (in.)
F	axial force, N (lb)
FS	factor of safety
G	elastic shear modulus, MPa (ksi)
g	gravitational constant, m/s^2 (in/s^2)
K_e	fatigue strength reduction factor
$(K_t)_a$	theoretical stress concentration factor in axial loading
$(K_t)_b$	theoretical stress concentration factor in bending
$(K_t)_t$	theoretical stress concentration factor in torsion

k_a	surface factor
k_b	size factor
k_c	reliability factor
k_d	temperature factor
$(k_e)_b$	fatigue stress concentration factor in bending
$(k_e)_t$	fatigue stress concentration factor in torsion
k_f	press-fitted collar factor
k_g	residual stress factor
k_h	corrosion factor
k_i	miscellaneous effects factor
L	length of solid circular shaft, m (in.)
M	bending moment, N-m (in-lb)
m	total number of bodies
N_f	number of cycles to failure at σ_f
N_i	number of cycles to failure under load i
n	shaft speed, rpm
n_i	number of loading cycles under load i
P_o	transmitted power, kW (hp)
q	notch sensitivity
r	notch radius, mm (in.)
T	torque, N-m (in-lb)
V	maximum transverse shear load, N (lb)
W_i	weight of i th body, N (lb)
Z	transverse-section modulus, m ³ (in ³)
Z_p	polar-section modulus, m ³ (in ³)
α	inside- to outside-diameter ratio, d_i/d_o
$\delta_{b,i}$	deflection due to bearing deflection under load W_i , m (in.)
δ_i	total static deflection under load W_i , m (in.)
$\delta_{s,i}$	deflection due to static shaft bending under load W_i , m (in.)
θ	torsional shaft deflection, deg
σ	bending stress, MPa (ksi)
σ_{ef}	effective nominal stress, MPa (ksi)
σ_f	corrected bending fatigue limit of shaft, MPa (ksi)
$\sigma_{f,t}$	corrected bending fatigue limit of shaft considering $(k_e)_t$ rather than $(k_e)_b$, MPa (ksi)
σ_f^*	bending or tensile fatigue limit of polished, unnotched test specimen without mean stress, MPa (ksi)
$\sigma_{f,m}^*$	bending or tensile fatigue limit of polished, unnotched test specimen with mean stress, MPa (ksi)

σ_f^*	true cyclic fracture strength or fatigue strength coefficient, MPa (ksi)
σ_u	ultimate tensile strength, MPa (ksi)
σ_y	yield tensile strength, MPa (ksi)
τ	shear stress, MPa (ksi)
τ_u	ultimate shear strength, MPa (ksi)
τ_y	yield shear strength, MPa (ksi)
ω_c	first critical shaft frequency, rad/s

Subscripts:

a	alternating or amplitude; half the total stress range
m	mean
max	maximum
min	minimum
nom	nominal
r	fully reversing

Static or Steady Loading

The state of stress to be considered is caused by torque transmitted to the shaft, bending of the shaft due to its weight or load, and axial forces imparted to the shaft. These three basic types or cases are given here.

Pure Torque

Case 1 considers pure torque. For a shaft transmitting power P_o at a rotational speed n , the transmitted torque T can be found from

$$\left. \begin{aligned} T(\text{N-m}) &= 9550 \frac{P_o(\text{kW})}{n(\text{rpm})} \\ \text{or} \\ T(\text{in-lb}) &= 63\,025 \frac{P_o(\text{hp})}{n(\text{rpm})} \end{aligned} \right\} \quad (1)$$

The relation between nominal shear stress τ_{nom} , torque T , and polar-section modulus Z_p is given by

$$\left. \begin{aligned} \tau_{\text{nom}}(\text{N/m}^2) &= \frac{T(\text{N-m})}{Z_p(\text{m}^3)} \\ \text{or} \\ \tau_{\text{nom}}(\text{lb/in}^2) &= \frac{T(\text{in-lb})}{Z_p(\text{in}^3)} \end{aligned} \right\} \quad (2)$$

For a solid circular shaft the nominal shear stress

$$\tau_{\text{nom}} = \frac{16T}{\pi d_o^3} B \quad (3)$$

where $B = 1$. For a hollow circular shaft

$$B = \frac{1}{1 - \alpha^4}$$

$$\alpha = \frac{d_i}{d_o}$$

where

d_o outside diameter

d_i inside diameter

Shear stress in noncircular shafts can be calculated from relations found in table I (ref. 3). The torsion and design of crankshafts are described in reference 4.

Simple Bending

Case 2 considers simple bending. For a given bending moment M , transverse-section modulus Z , and nominal stress in bending σ_{nom}

$$M = \sigma_{\text{nom}} Z$$

For a circular shaft

$$\sigma_{\text{nom}} = \frac{32M}{\pi d_o^3} B \quad (4)$$

Combined Torsion, Bending, and Axial Loading

Case 3 considers combined torsion, bending, and axial loading on a circular shaft. When a shaft is subjected to torsion and bending, the induced stresses are larger than the direct stress due to T and M alone. The effective nominal stress σ_{ef} is

$$\sigma_{\text{ef}} = \frac{32}{\pi d_o^3} B \left\{ \left[M + \frac{Fd_o}{8} (1 + \alpha^2) \right]^2 + \frac{3}{4} T^2 \right\}^{1/2} \quad (5)$$

where F is axial force.

In terms of static or steady-state stress failure, a ductile metal is usually considered to have failed when it has suffered elastic failure, that is, when marked plastic deformation has begun. For ductile metals under static or steady loading, local yielding due to stress concentrations, such as small holes, notches, or fillets, is generally not troublesome. This is true provided that the volume of

the material affected and its location do not seriously reduce the strength of the member as a whole. Local plastic yielding of certain highly stressed elements permits some degree of stress relieving to occur and passes part of the stress on to adjacent elements within the member. Under these circumstances the local stress concentration factor can be neglected. Failure will generally occur when the effective stress σ_{ef} exceeds the yield strength of the bulk material σ_y . Thus for ductile metals where local yielding at stress concentration is acceptable, the shaft diameter (or outside diameter) can be found from

$$d_o^3 = \frac{\text{FS}}{\sigma_y} \frac{32}{\pi} B \left\{ \left[M + \frac{Fd_o}{8} (1 + \alpha^2) \right]^2 + \frac{3}{4} T^2 \right\}^{1/2} \quad (6)$$

where the factor of safety FS has been introduced for design conservatism. (The value to use for FS is based on judgment. It depends on the consequences of failure, that is, cost, time, safety, etc. Some factors to consider when selecting a value for FS are how well the actual loads, operating environment, and material strength properties are known, as well as possible inaccuracies of the calculation method. Values typically range from 1.3 to 6 depending on the confidence in the prediction technique and the criticality of the application. Unless experience or special circumstances dictate it, the use of FS values of less than 1.5 is not normally recommended.)

Brittle metals, such as cast iron, are likely to crack rather than yield locally at stress concentration points. These cracks can propagate through the member and cause shaft fracture. For the design of shafts made of metals with low ductility or fracture toughness, it is customary to apply theoretical stress concentration factors K_t to account for this effect. Because brittle metals experience fracture failure rather than plastic deformation, it is also customary to use the ultimate tensile strength of the material σ_u as the limiting strength factor. The diameters of shafts made from brittle metals can be found from

$$d_o^3 = \frac{\text{FS}}{\sigma_u} \frac{32}{\pi} B \left\{ \left[(K_t)_b M + (K_t)_a \frac{Fd_o}{8} (1 + \alpha^2) \right]^2 + \frac{3}{4} \left[(K_t)_t T \right]^2 \right\}^{1/2} \quad (7)$$

where

$(K_t)_b$ theoretical stress concentration factor in bending

$(K_t)_a$ theoretical stress concentration factor in axial loading

$(K_t)_t$ theoretical stress concentration factor in torsion

TABLE I.—SHAFT DATA^a

[From ref. 3.]

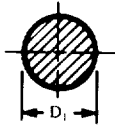
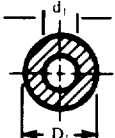
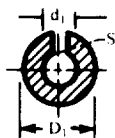
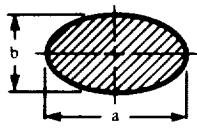
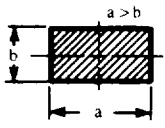
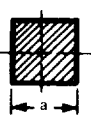
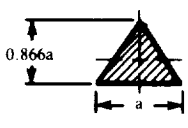

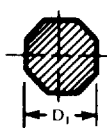
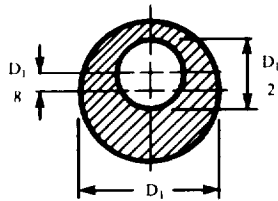
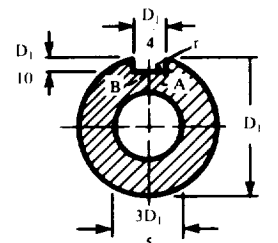
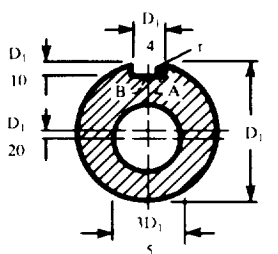
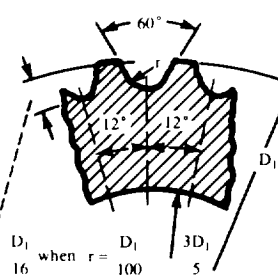
Cross section of shaft	Equivalent length of circular bar of diameter D	Maximum shear stress
	$L = L_1 D^4 \left(\frac{1}{D_1^4} \right)$	$\tau = \frac{5.1 T}{D_1^3}$ at periphery
	$L = L_1 D^4 \left(\frac{1}{D_1^4 - d_1^4} \right)$	$\tau = \frac{5.1 D_1 T}{D_1^4 - d_1^2}$ at periphery
	$L = L_1 D^4 \left[\frac{1.5}{(D_1 + d_1)(D_1 - d_1)^3} \right]$	$\tau = \frac{7.6 T}{(D_1 + d_1)(D_1 - d_1)^2}$
	$L = L_1 D^4 \left(\frac{a^2 + b^2}{2a^3 b^3} \right)$	$\tau = \frac{5.1 T}{ab^2}$ at X
	$L = L_1 D^4 \left(\frac{a^2 + b^2}{3.1 a^3 b^3} \right)$	$\tau = \left(\frac{15a + 9b}{5a^2 b^2} \right) T$ at X
	$L = L_1 D^4 \left(\frac{1}{1.43 a^4} \right)$	$\tau = \frac{4.8 T}{a^3}$ at X
	$L = L_1 D^4 \left(\frac{4.53}{a^4} \right)$	$\tau = \frac{20 T}{a^3}$ at X
	$L = L_1 D^4 \left(\frac{1}{1.18 D_1^4} \right)$	$\tau = \frac{5.3 T}{D_1^3}$ at X
	$L = L_1 D^4 \left(\frac{1}{1.10 D_1^4} \right)$	$\tau = \frac{5.4 T}{D_1^3}$ at X

TABLE I.—Concluded

Cross section of shaft	Equivalent length of circular bar of diameter D	Maximum shear stress																											
	$L = L_1 D^4 \left(\frac{1.16}{D_1^4} \right)$	$\tau = \frac{8.1T}{D_1^3} \text{ at } X$																											
	$L = L_1 D^4 \left(\frac{K}{D_1^4} \right)$ <table border="1" data-bbox="698 798 868 976"> <thead> <tr> <th>r</th> <th>K</th> </tr> </thead> <tbody> <tr> <td>$D_1/100$</td> <td>1.28</td> </tr> <tr> <td>$D_1/50$</td> <td>1.27</td> </tr> <tr> <td>$D_1/25$</td> <td>1.26</td> </tr> <tr> <td>$D_1/15$</td> <td>1.24</td> </tr> </tbody> </table>	r	K	$D_1/100$	1.28	$D_1/50$	1.27	$D_1/25$	1.26	$D_1/15$	1.24	$\tau = \frac{K_1 T}{D_1^3}$ <table border="1" data-bbox="990 777 1242 976"> <thead> <tr> <th rowspan="2">r</th> <th colspan="2">K_1</th> </tr> <tr> <th>At A</th> <th>At B</th> </tr> </thead> <tbody> <tr> <td>$D_1/100$</td> <td>31.5</td> <td>13.4</td> </tr> <tr> <td>$D_1/50$</td> <td>19.7</td> <td>13.0</td> </tr> <tr> <td>$D_1/25$</td> <td>13.5</td> <td>12.6</td> </tr> <tr> <td>$D_1/15$</td> <td>11.0</td> <td>11.7</td> </tr> </tbody> </table>	r	K_1		At A	At B	$D_1/100$	31.5	13.4	$D_1/50$	19.7	13.0	$D_1/25$	13.5	12.6	$D_1/15$	11.0	11.7
r	K																												
$D_1/100$	1.28																												
$D_1/50$	1.27																												
$D_1/25$	1.26																												
$D_1/15$	1.24																												
r	K_1																												
	At A	At B																											
$D_1/100$	31.5	13.4																											
$D_1/50$	19.7	13.0																											
$D_1/25$	13.5	12.6																											
$D_1/15$	11.0	11.7																											
	$L = L_1 D^4 \left(\frac{K}{D_1^4} \right)$ <table border="1" data-bbox="698 1144 868 1323"> <thead> <tr> <th>r</th> <th>K</th> </tr> </thead> <tbody> <tr> <td>$D_1/100$</td> <td>1.29</td> </tr> <tr> <td>$D_1/50$</td> <td>1.29</td> </tr> <tr> <td>$D_1/25$</td> <td>1.28</td> </tr> <tr> <td>$D_1/15$</td> <td>1.26</td> </tr> </tbody> </table>	r	K	$D_1/100$	1.29	$D_1/50$	1.29	$D_1/25$	1.28	$D_1/15$	1.26	$\tau = \frac{K_1 T}{D_1^3}$ <table border="1" data-bbox="990 1113 1242 1323"> <thead> <tr> <th rowspan="2">r</th> <th colspan="2">K_1</th> </tr> <tr> <th>At A</th> <th>At B</th> </tr> </thead> <tbody> <tr> <td>$D_1/100$</td> <td>13.0</td> <td>8.7</td> </tr> <tr> <td>$D_1/50$</td> <td>9.7</td> <td>8.6</td> </tr> <tr> <td>$D_1/25$</td> <td>8.6</td> <td>8.5</td> </tr> <tr> <td>$D_1/15$</td> <td>8.3</td> <td>8.4</td> </tr> </tbody> </table>	r	K_1		At A	At B	$D_1/100$	13.0	8.7	$D_1/50$	9.7	8.6	$D_1/25$	8.6	8.5	$D_1/15$	8.3	8.4
r	K																												
$D_1/100$	1.29																												
$D_1/50$	1.29																												
$D_1/25$	1.28																												
$D_1/15$	1.26																												
r	K_1																												
	At A	At B																											
$D_1/100$	13.0	8.7																											
$D_1/50$	9.7	8.6																											
$D_1/25$	8.6	8.5																											
$D_1/15$	8.3	8.4																											
	$L = L_1 D^4 \left(\frac{K}{D_1^4} \right)$ <table border="1" data-bbox="698 1501 868 1680"> <thead> <tr> <th>r</th> <th>K</th> </tr> </thead> <tbody> <tr> <td>$D_1/100$</td> <td>1.86</td> </tr> <tr> <td>$D_1/75$</td> <td>1.79</td> </tr> <tr> <td>$D_1/50$</td> <td>1.72</td> </tr> <tr> <td>$D_1/40$</td> <td>1.64</td> </tr> </tbody> </table>	r	K	$D_1/100$	1.86	$D_1/75$	1.79	$D_1/50$	1.72	$D_1/40$	1.64	$\tau = \frac{K_1 T}{D_1^3}$ <table border="1" data-bbox="1031 1501 1201 1680"> <thead> <tr> <th>r</th> <th>K_1</th> </tr> </thead> <tbody> <tr> <td>$D_1/100$</td> <td>20.0</td> </tr> <tr> <td>$D_1/75$</td> <td>15.5</td> </tr> <tr> <td>$D_1/50$</td> <td>14.6</td> </tr> <tr> <td>$D_1/40$</td> <td>13.8</td> </tr> </tbody> </table>	r	K_1	$D_1/100$	20.0	$D_1/75$	15.5	$D_1/50$	14.6	$D_1/40$	13.8							
r	K																												
$D_1/100$	1.86																												
$D_1/75$	1.79																												
$D_1/50$	1.72																												
$D_1/40$	1.64																												
r	K_1																												
$D_1/100$	20.0																												
$D_1/75$	15.5																												
$D_1/50$	14.6																												
$D_1/40$	13.8																												

^a L = length of solid, circular shaft of diameter D having the same torsional rigidity as length L_1 of the actual shaft; T = torque transmitted by shaft.

Typical values of K_t for shafts with fillets and holes are given in figures 1 and 2. Factors for numerous other cases appear in reference 5.

It is worth noting that applying the full value of K_t in the design of shafts made of some brittle metals may not be justified from strictly a strength standpoint. However, it is usually prudent to use full K_t values in view of a brittle metal's poor resistance to shock loading. A second point to be made is that surface-hardened ductile steel shafts can exhibit brittle behavior at stress concentration points. Although cracks may stop at the softer core interface, some reduction in strength will still occur. This reduction in strength should be taken into account when selecting FS values.

Some shafts can fail under heavy transverse shear loading. For short, solid shafts having only transverse shear loading, the shaft diameter is given by

$$d_o = \frac{1.7V}{\tau_y/FS} \quad (8)$$

where

τ_y shear yield strength (0.577 σ_y for most steels)
 V maximum transverse shear load

Shafts with a high degree of hollowness, or in other words tubes, may fail from buckling rather than from stress. Reference 6 should be consulted.

Fluctuating Loads

Ductile machine elements subjected to repeated fluctuating stresses above their endurance strength but below their yield strength will eventually fail from fatigue. The insidious nature of fatigue is that it occurs without visual warning at bulk operating stresses below plastic deformation. Shafts sized to avoid fatigue will usually be strong enough to avoid elastic failure unless severe transient or shock overloads occur.

Failure from fatigue is statistical in nature inasmuch as the fatigue life of a particular specimen cannot be precisely predicted but rather the likelihood of failure is predicted on the basis of a large population of specimens. For a group of specimens or parts made to the same specification the key fatigue variables would be the effective operating stress, the number of stress cycles, and the volume of material under stress. Since the effective stresses are usually highest at points along the surface where discontinuities occur, such as keyways, splines, and fillets, these are the points from which fatigue cracks are most likely to emanate. However, each volume of material under stress carries with it a finite probability of failure. The product of these elemental probabilities (the "weakest link" criterion) yields the

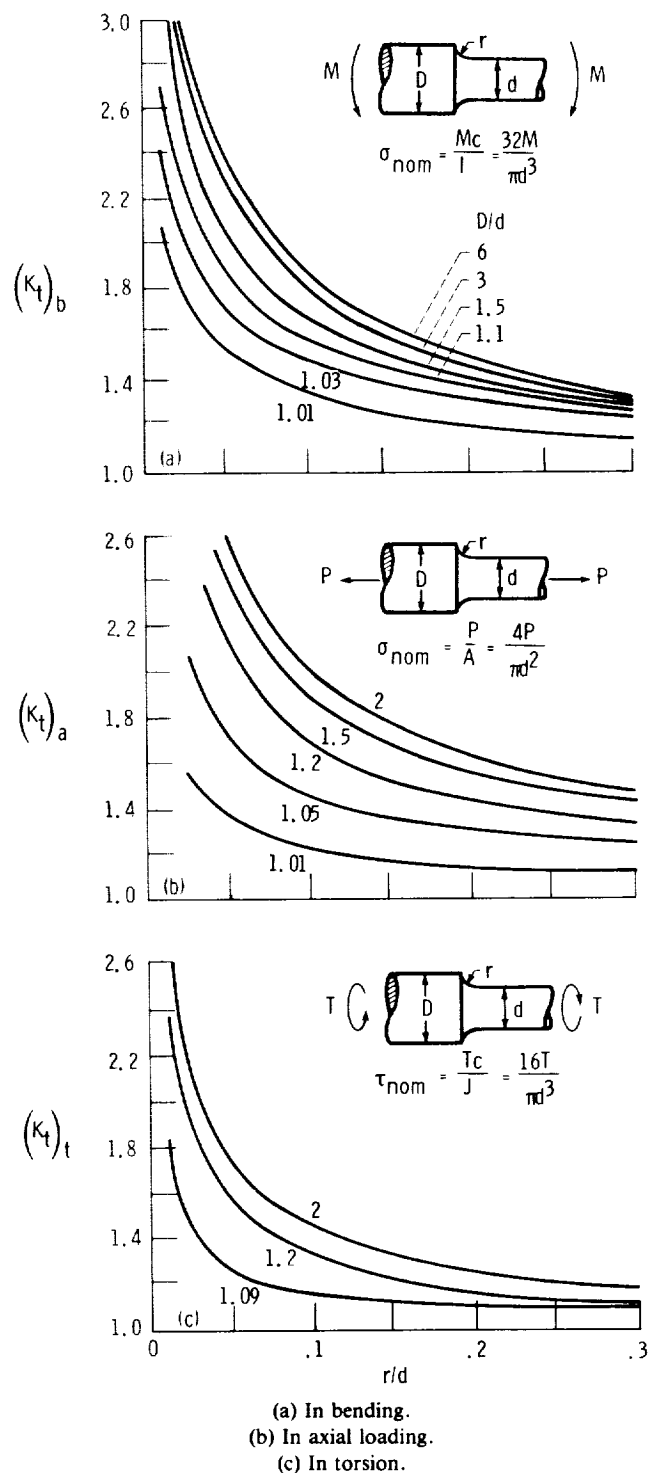


Figure 1.—Theoretical stress concentration factors for shaft with fillet. (From ref. 8.)

likelihood of failure for the entire part for a given number of loading cycles.

At present there is no unified, statistical failure theory to predict shafting fatigue. However, reasonably accurate life estimates can be derived from general design equations coupled with bench fatigue data and material

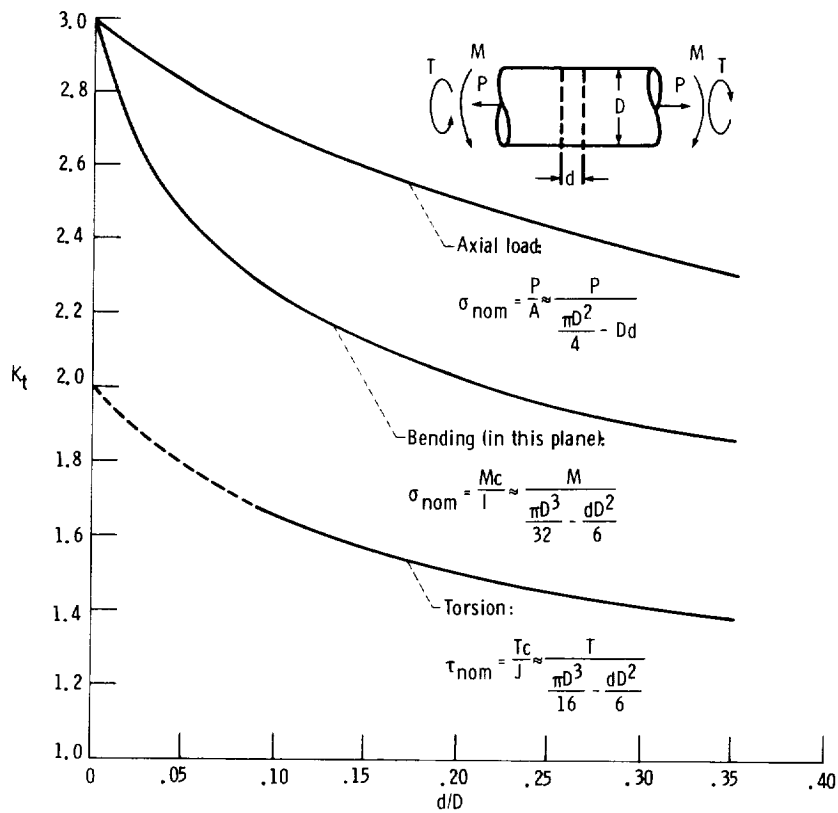


Figure 2.—Theoretical stress concentration factors for shaft with radial hole. (From ref. 8.)

static properties. Fatigue test data are often obtained either on a rotating-beam tester under the conditions of reversed bending or on an axial fatigue tester. The data generated from these machines are usually plotted in the form of stress-life (S-N) diagrams. On these diagrams the bending stress at which the specimens did not fail after some high number of stress cycles, usually 10^6 to 10^7 cycles for steel, is commonly referred to as the fatigue limit σ_f . For mild steels it is the stress at which the S-N curve becomes nearly horizontal. This seems to imply that operating stresses below the fatigue limit will lead to “infinite” service life. However, this is misleading since *no part can have a 100 percent probability of survival*. In fact, fatigue limit values determined from S-N diagrams normally represent the mean value of the failure distribution due to test data scatter. Statistical corrections must be applied for designs requiring high reliabilities, as will be discussed. Furthermore many high-strength steels, nonferrous materials, and even mild steel in a corrosive environment do not exhibit a distinct fatigue limit. In view of this it is best to consider that the fatigue limit represents a point of *very long life* ($> 10^6$ cycles).

Up until now the design equations given are for shafts with steady or quasi-steady loading. However, most shafts rotate with gear, sprocket, or pulley radial loads and thereby produce fluctuating stresses. Fluctuating stresses can be broken into two components: an alternating stress component σ_a superimposed on a mean

stress component σ_m . Under the special circumstance when σ_m is zero, σ_a is said to be a fully reversing stress σ_r .

The formulas that follow are for solid circular shafts. These formulas can also be applied with caution to hollow shafting. Their applicability to thin-wall shafts (tubes) has not yet been established.

Simple Loading

The loading is considered to be simple when only one kind of stress exists, that is, only either fluctuating bending, torsion, or tension.

Several failure relations have been proposed for simple loading, but the modified Goodman line is, perhaps, the most widely used. It is given by

$$\frac{\sigma_a}{\sigma_f} + \frac{\sigma_m}{\sigma_u} = 1 \quad (9)$$

where

- σ_u ultimate tensile or torsional strength
- σ_f fatigue limit of the shaft, that is, the fatigue limit of the shaft material after it has been corrected by certain application factors known to affect fatigue strength, such as those due to surface finish, size, or stress concentration

These fatigue modifying factors are addressed later in this report.

Fluctuating Bending

For the case of a fluctuating bending moment load consisted of an alternating bending moment M_a superimposed on a steady bending moment M_m , the appropriate solid shaft diameter for long life (at least 10^6 cycles) can be found from

$$d^3 = \frac{32(\text{FS})}{\pi} \left(\frac{M_a}{\sigma_f} + \frac{M_m}{\sigma_u} \right) \quad (10)$$

where

$$M_m = \frac{M_{\max} + M_{\min}}{2} \quad (11)$$

$$M_a = \frac{M_{\max} - M_{\min}}{2}$$

Fluctuating Torsion

For the case of a fluctuating torsional load consisting of an alternating torque T_a superimposed on a steady torque T_m , the shaft diameter can be found from

$$d^3 = \frac{16(\text{FS})}{\pi} \left(\frac{T_a}{\tau_f} + \frac{T_m}{\tau_u} \right) \quad (12)$$

where

τ_f reversed torsional fatigue limit
 τ_u ultimate shear strength

and where expressions similar to equation (11) apply for T_a and T_m . From the maximum distortion-energy theory of failure the shear strength and torsional endurance limit properties of a material are approximately related to the tensile properties by

$$\tau_f = \frac{\sigma_f}{\sqrt{3}}$$

$$\tau_u = \frac{\sigma_u}{\sqrt{3}}$$

Making these substitutions into equation (12) gives

$$d^3 = \frac{16\sqrt{3}}{\pi} (\text{FS}) \left(\frac{T_a}{\sigma_{f,t}} + \frac{T_m}{\sigma_u} \right) \quad (13)$$

where $\sigma_{f,t}$ is the fatigue limit of a shaft considering a torsional rather than a bending fatigue stress concentration factor.

A large amount of fatigue data (ref. 7) is available on various metals including steel, iron, aluminum, and copper. It is instructive to note that these data show the torsional fatigue strength of smooth, notch-free members to be unaffected by the presence of a mean torsional stress component up to and slightly beyond the torsional yield strength of the material. However, when significant stress raisers are present, the more common case, test data cited by Juvinal (ref. 8) indicate that the torsional fatigue strength properties of the shaft member will be reduced by the presence of a mean or steady torsional stress component in accordance with equation (9). Juvinal (ref. 8) attributes this to the observation that the state of stress at the point of stress concentration deviates from that of pure shear. Thus equation (13) is recommended except when the shaft to be designed is *substantially free from points of stress concentration*, in which case the following can be used:

$$d^3 = \frac{16\sqrt{3}}{\pi} (\text{FS}) \left(\frac{T_a}{\sigma_{f,t}} \right) \quad (14)$$

To avoid possible yielding failure, the shaft diameter should be no smaller than

$$d^3 = \frac{16\sqrt{3}}{\pi} (\text{FS}) \left(\frac{T_a + T_m}{\sigma_y} \right) \quad (15)$$

Fatigue Under Combined Stresses

For applications where a simple fluctuating stress of the same kind is acting (e.g., an alternating bending stress superimposed on a steady bending stress), the Goodman failure line method just described provides an acceptable design. However, most power-transmitting shafts are subjected to a combination of reversed bending stress (a rotating shaft with constant moment loading) and steady or nearly steady torsional stress. Although a large body of test data has been generated for the simple stress condition, such as pure tensile, flexural, or torsional stress, little information has been published for the combined bending and torsional stress condition. However, some cyclic bending and steady torsional fatigue test data (ref. 9) for alloy steel show a reduction in reversed bending fatigue strength with mean torsion stress according to the elliptical relation

$$\left(\frac{\sigma_r}{\sigma_f} \right)^2 + \left(\frac{\tau_m}{\tau_y} \right)^2 = 1 \quad (16)$$

Reversed Bending with Steady Torsion

From the failure relation given in equation (16), the following formula can be used to size solid or hollow shafts under reversed bending M_r and steady torsional T_m loading with negligible axial loading:

$$d_0^3 = \frac{32(\text{FS})}{\pi} B \left[\left(\frac{M_r}{\sigma_f} \right)^2 + \frac{3}{4} \left(\frac{T_m}{\sigma_y} \right)^2 \right]^{1/2} \quad (17)$$

Equation (17) is the basic shaft design equation proposed for the soon-to-be-released ASME Standard B106.1M, Design of Transmission Shafting (ref. 9). It can also be derived theoretically from the distortion-energy failure theory as applied to fatigue loading.

Fluctuating Bending Combined with Fluctuating Torsion

In the general case when both the bending and torsional moments acting on the shaft are fluctuating, the safe shaft diameter, according to the distortion-energy theory can be found from

$$d_0^3 = \frac{32(\text{FS})}{\pi} B \left[\left(\frac{M_m}{\sigma_u} + \frac{M_a}{\sigma_f} \right)^2 + \frac{3}{4} \left(\frac{T_m}{\sigma_y} + \frac{T_a}{\sigma_{f,t}} \right)^2 \right]^{1/2} \quad (18)$$

Fatigue Life Modifying Factors

In equations (10), (13), (17), and (18) the *fatigue limit of the shaft* to be designed is almost always different from the fatigue limit of the highly polished, notch-free fatigue test specimen listed in material property tables. A number of service factors that are known to affect fatigue strength have been identified. These factors can be used to modify the uncorrected fatigue limit of the test specimen σ_f^* as follows:

$$\sigma_f = k_a k_b k_c k_d (k_e)_b k_f k_g k_h k_i \sigma_f^* \quad (19)$$

or

$$\sigma_{f,t} = k_a k_b k_c k_d (k_e)_t k_f k_g k_h k_i \sigma_f^*$$

where

- σ_f corrected bending fatigue limit of shaft
- $\sigma_{f,t}$ corrected bending fatigue limit of shaft considering $(k_e)_t$ rather than $(k_e)_b$
- σ_f^* bending or tensile fatigue limit of polished, unnotched test specimen without mean stress

- k_a surface factor
- k_b size factor
- k_c reliability factor
- k_d temperature factor
- $(k_e)_b$ fatigue stress concentration factor in bending
- $(k_e)_t$ stress concentration factor in torsion
- k_f press-fitted collar factor
- k_g residual stress factor
- k_h corrosion factor
- k_i miscellaneous effects factor

Table II lists representative σ_f^* values for selected steels obtained from axial fatigue tests along with other material fatigue properties. Fatigue limit values from axial tests normally tend to be somewhat smaller than those obtained in bending, but the differences are usually within the scatter caused by other test variables. The probable reason for this is that the highly stressed region extends across the axial specimen's entire cross section rather than being confined to the outer fibers as in the case of specimens tested in bending. Since more material is being stressed with the axial specimen, there is a corresponding increase in the probability of encountering a fatigue-initiating defect. Although bending fatigue strength values are preferred, it is not unreasonable to use those from axial tests for the design of shafts. In the event that actual user or steel supplier test data are unavailable, a rough rule of thumb for steel is

$$\left. \begin{aligned} \sigma_f^* &\approx 0.5 \sigma_u & \sigma_u &\leq 1400 \text{ MPa (200 ksi)} \\ \sigma_f^* &\approx 700 \text{ MPa (100 ksi)} & \sigma_u &> 1400 \text{ MPa (200 ksi)} \end{aligned} \right\} (20)$$

It is important to remember that σ_f^* values in table II do not represent final design values but must be corrected by the factors given in equation (19).

Surface Factor k_a

Since the shaft surface is the most likely place for fatigue cracks to start, the surface condition significantly affects the fatigue limit, as shown in figure 3. This figure is based on a compilation of test data from several investigations for a variety of ferrous metals and alloys (ref. 10). The figure shows that the endurance characteristics of the higher tensile strength steels are more adversely affected by poorer surface conditions. Furthermore it shows that surface decarburization, which often accompanies forging, can severely reduce fatigue strength. Most, if not all, of the strength reduction due to surface condition can be recovered by cold rolling, shot peening, and other means of inducing residual compressive stress into the surface, as discussed later.

TABLE II.—REPRESENTATIVE STRENGTH AND FATIGUE PROPERTIES OF SELECTED STEELS BASED ON TEST SPECIMEN DATA WITHOUT MEAN STRESSES

[From refs. 21 and 22. Values listed are typical. Specific values should be obtained from the steel producer.]

SAE specification	Brinell hardness number, BHN	Process	Ultimate tensile strength, σ_u		Yield tensile strength, σ_y		Fatigue strength coefficient, σ_f'		Fatigue ^a strength exponent, b	Bending or tensile fatigue limit at 10^6 cycles, σ_f^*	
			MPa	ksi	MPa	ksi	MPa	ksi		MPa	ksi
1005-1009	125	Cold-drawn sheet	414	60	400	58	538	78	0.073	244	35
1005-1009	90	Hot-rolled sheet	345	50	262	38	641	93	.109	202	29
1015	80	Normalized	414	60	228	33	827	120	.11	186	27
1018	126	Cold-drawn bar	441	64	372	54	---	---	---	---	---
1020	108	Hot-rolled plate	441	64	262	38	896	130	.12	208	30
1022	137	Cold-drawn bar	476	69	400	58	---	---	---	---	---
1040	170	Cold-drawn bar	586	85	490	71	---	---	---	---	---
1040	225	As forged	621	90	345	50	1538	223	.14	233	33
1045	225	Quenched and tempered	724	105	634	92	1227	178	.095	323	47
1045	390	↓	1344	195	1276	185	1586	230	.074	547	79
1045	500	↓	1827	265	1689	245	2275	330	.08	715	104
1045	595	↓	2241	325	1862	270	2723	395	.081	843	122
1050	197	Cold-drawn bar	690	100	579	84	---	---	---	---	---
1140	170	Cold-drawn bar	607	88	510	74	---	---	---	---	---
1144	305	Drawn at temperature	1034	150	1020	148	1586	230	.09	454	66
1541F	290	Quenched, tempered, and forged	951	138	889	129	1276	185	.076	435	63
4130	258	Quenched and tempered	896	130	779	113	1276	185	.083	404	59
4130	365	Quenched and tempered	1427	207	1358	197	1696	246	.081	532	77
4140	310	Quenched and tempered; drawn at temperature	1076	156	965	140	1827	265	.08	619	90
4142	310	Drawn at temperature	1062	154	1048	152	1448	210	.10	366	53
4142	380	Quenched and tempered	1413	205	1379	200	1827	265	.08	574	83
4142	450	Quenched, tempered, and deformed	1931	280	1862	270	2103	305	.09	572	83
4340	243	Hot rolled and annealed	827	120	634	92	1200	174	.095	337	49
4340	409	Quenched and tempered	1469	213	1372	199	1999	290	.091	550	80
4340	350	Quenched and tempered	1241	180	1172	170	1655	240	.076	567	82
5160	430	Quenched and tempered	1669	242	1531	222	1931	280	.071	709	103

^aFatigue strength exponent is listed as positive quantity.

As stated in reference 10, the ground surface category includes all types of surface finishing that do not affect the fatigue limit by more than 10 percent. Polished, ground, honed, lapped, or superfinished shafts are included in this ground category as well as commercial shafts that are turned, ground, and polished or turned and polished. The machined surface category includes shafts that are either rough, finish machined, or unfinished and cold drawn with roughnesses between 1.6 and 6.3 μm (63 and 250 $\mu\text{in.}$). The hot-rolled category covers surface conditions encountered on hot-rolled shafts that have slight irregularities and some included oxide and scale defects with partial surface decarburization. The as-forged category includes shafts with larger surface irregularities and included oxide and scale defects with total surface decarburization.

Size Factor k_b

There is considerable experimental evidence that the bending and torsional fatigue strengths of large shafts can be significantly less than those of the small test specimens (typically 7.6 mm or 0.30 in. in diameter) that are used to generate fatigue data (refs. 11 and 12). The size effect is attributed the greater volume of material under stress and thus the greater likelihood of encountering a potential fatigue-initiating defect in the material's metallurgical structure. Also the heat treatment of large parts can produce a metallurgical structure that neither is as uniform nor has as fine a grain structure as that obtained with smaller parts. Another factor is that smaller shafts have a higher stress gradient; that is, the rate of stress change with depth is greater (ref. 11).

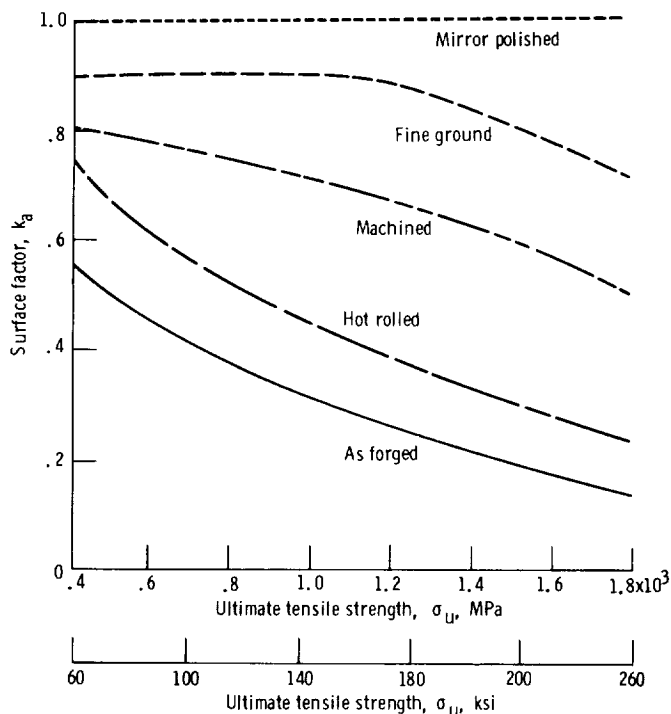


Figure 3.—Surface factor as a function of surface condition and ultimate tensile strength. (Test data from ref. 10.)

Figure 4 shows the effect of size on the bending fatigue strength of unnotched, polished, steel test specimens up to 5 cm (2 in.) in diameter from many investigations. The curve in this figure is based on Kuguel's theory (ref. 11), which relates the reduction in fatigue strength to the increase in the volume of material under 95 percent of the peak stress. The Kuguel expression can be written as

$$k_b = \left(\frac{d}{0.76} \right)^{-0.068}$$

where d is the shaft diameter in millimeters

or

$$k_b = \left(\frac{d}{0.3} \right)^{-0.068} \quad (21)$$

where d is the shaft diameter in inches.

For larger shafts, that is, above 50 mm (2 in.) in diameter, there are insufficient data for establishing a definitive formula. The few relevant tests for 150- and 216-mm (6- and 8.5-in.) diameter, plain carbon steel specimens in rotating bending have shown a considerable reduction in fatigue strength (ref. 12). The following expression, in the absence of actual data for the shaft to be designed, should provide a reasonable estimate of the size factor for shafts between 50 and 250 mm (2 and 10 in.) in diameter:

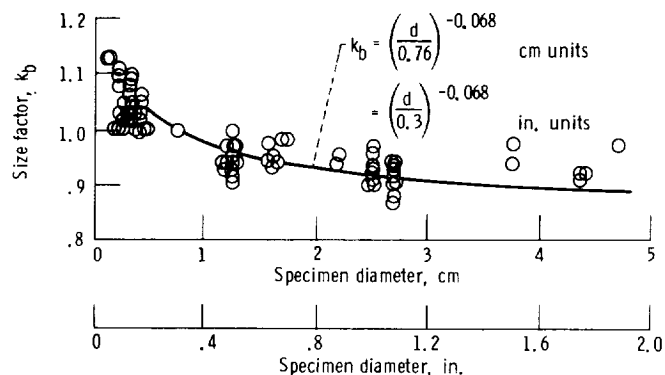


Figure 4.—Size factor as a function of specimen diameter. Data for unnotched, polished steel specimens having yield tensile strengths of 50 to 165 ksi were compiled from several sources. (From ref. 8.)

$$k_b = 1.85 d^{-0.19} \text{ mm} = d^{-0.19} \text{ in.} \quad (22)$$

Reliability Factor k_c

Even under well-controlled test conditions the unavoidable variability in the preparation of test specimens and their metallurgical structure clearly causes a variability in their measured fatigue strengths. Fatigue limit data published in standard design references usually represent a mean value of endurance for the sample of test specimens. If the failure distribution is taken to be normally distributed or nearly so, these data also approximately represent the median strength, that is, the stress level at which half of the population will fail. Most designs require a much higher survival rate than 50 percent, which corresponds to the probability that at least half of the population will not fail in service. Consequently fatigue limit values must be reduced by some amount to increase reliability. The amount of this reduction depends on the failure distribution curve and required reliability.

In reference 13 rotating bending fatigue data for SAE 4340 and 4350 steels ranging from 970 to 2070 MPa (140 to 300 ksi) were statistically analyzed. These data exhibited a reasonably normal or Gaussian failure distribution with a standard deviation of 5 to 8 percent of the mean fatigue limit strength. Values of k_c corresponding to these values of standard deviation can be computed by standard statistical methods. These k_c values are listed in table III. If statistical failure distribution information is available for the shaft material selected, of course, it is to be used (e.g., see refs. 8, 16, and 19 on applying statistical methods to fatigue design). However, in the absence of actual test data the k_c values corresponding to an 8-percent standard deviation are normally recommended (ref. 13).

As a word of caution, correction factors for very high levels of reliability, say 99 percent and above, are quite sensitive to the type of failure distribution assumed and its dispersion. Accordingly, when specific component

TABLE III.—RELIABILITY
FACTOR k_c

Shaft nominal reliability, percent survival	Standard deviation, ^a percent of mean fatigue limit strength	
	5	8
	Reliability factor, k_c	
50	1.0	1.0
90	.936	.897
95	.918	.868
99	.884	.814
99.9	.864	.753
99.99	.814	.702

^aA standard deviation of 8 percent is recommended if actual test data are unavailable.

failure data are lacking, the k_c values listed in table III for these very high reliability levels should be viewed as more of a guide than in absolute terms.

Temperature Factor k_d

Test data (refs. 7 and 14) indicate that the fatigue limits of carbon and alloy steel are relatively unaffected by operating temperatures from approximately -73° to 316° C (-100° to 600° F) (table IV). For this temperature range $k_d = 1$ is recommended. At lower temperatures (to -129° C, or -200° F) carbon and alloy steels possess significantly greater bending fatigue strength. As the temperature is increased to approximately 427° C (800° F), carbon steels actually show a small improvement in fatigue strength relative to room-temperature values, but

alloy steel (SAE 4340) shows a slight decrease in fatigue strength. At temperatures above 427° C (800° F) the fatigue resistance of both types of steel drops sharply as the effects of creep and loss of material strength properties become more pronounced. For applications outside the normal temperature range the fatigue properties for the shaft material should be ascertained from published or user-generated test data. Reference 7 should provide some guidance on k_d values for typical steels.

Fatigue Stress Concentration Factor k_e

Experience has shown that a shaft fatigue failure almost always occurs at a notch, hole, keyway, shoulder, or other discontinuity where the effective stresses have been amplified. These are the obvious locations where the shaft should be first analyzed, particularly in regions of high stress. The effect of a stress concentration on the fatigue limit of the shaft is represented by the fatigue stress concentration factor k_e , where

$$k_e = \frac{\text{Fatigue limit of notched specimen}}{\text{Fatigue limit of specimen free of notches}} = \frac{1}{K_e} \quad (23)$$

and K_e is the fatigue strength reduction factor.

Experimental fatigue data (ref. 5) indicate that low-strength steels are significantly less sensitive to notches or other stress raisers than high-strength steels — as reflected by the notch sensitivity parameter q shown in figure 5. The fatigue strength reduction factor K_e can be related to the theoretical (static) stress concentration factor K_t as follows:

TABLE IV.—TEMPERATURE FACTOR - FATIGUE PROPERTIES AS RELATED TO ROOM-TEMPERATURE (23° C; 70° F) PROPERTIES

[From refs. 7 and 14.]

Steel (condition)	Temperature, $^\circ$ C ($^\circ$ F)								
	-129 (-200)	-73 (-100)	-18 (0)	23 (70)	93 (200)	204 (400)	316 (600)	427 (800)	538 (1000)
	Temperature factor, k_d								
SAE 1035	1.7	1.3	1.1	1.0	1.0	1.2	1.4	1.3	0.8
SAE 1060	1.5	1.2	1.1	1.0	1.0	1.1	1.2	1.0	.2
SAE 4340	1.3	1.1	1.0	1.0	.9	.9	.9	.8	.6
SAE 4340 (notched)	---	---	---	1.0	---	---	.9	.9	.8
0.17 Percent carbon	---	---	---	1.0	1.0	1.0	1.4	1.2	.6
SAE 4340	---	---	---	1.0	---	---	1.0	1.0	.5
Carbon steel	---	1.3	---	1.0	---	---	---	---	---
Carbon steel (notched)	---	1.1	---	1.0	---	---	---	---	---
Alloy steel (notched)	---	1.1	---	1.0	---	---	---	---	---

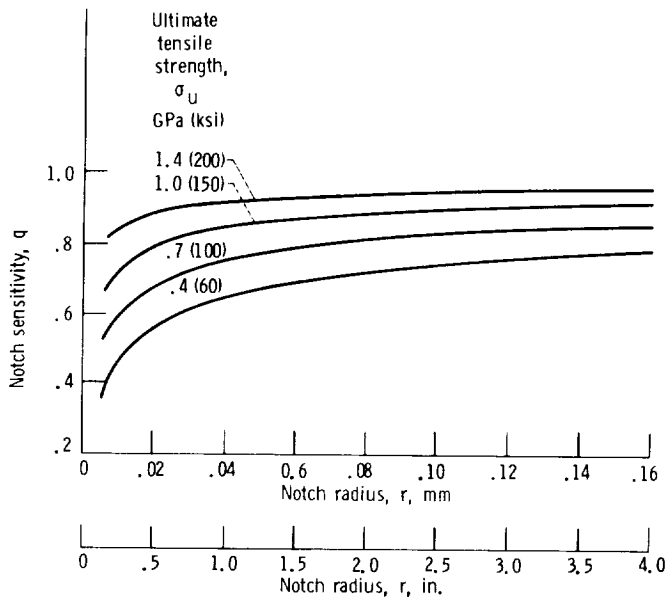


Figure 5.—Notch sensitivity as a function of notch radius and ultimate tensile strength for steels subjected to reverse bending or reverse axial loads. (From refs. 5 and 8.)

$$K_e = 1 + q(K_t - 1) \quad (24)$$

The appropriate K_t to be used in equation (24) is the one that corresponds to the type of cyclic loading that is present. Thus for a cyclic bending stress the bending fatigue stress factor is

$$(k_e)_b = \frac{1}{1 + q[(K_t)_b - 1]} \quad (25)$$

Similarly for cyclic torsion

$$(k_e)_t = \frac{1}{1 + q[(K_t)_t - 1]} \quad (26)$$

Representative values of $(K_t)_b$ and $(K_t)_t$ for shafts with fillets and holes are given in figures 1 and 2. A compendium of K_t values for a wide variety of geometries appears in reference 5. Typical design values of $(k_e)_b$ and $(k_e)_t$ for steel shafts with keyways are presented in table V (ref. 15).

Press-Fitted Collar Factor k_f

A common method of attaching gears, bearings, couplings, pulleys, and wheels to shafts or axles is through the use of an interference fit. The change in section creates a point of stress concentration at the face of the collar. This stress concentration coupled with the fretting action of the collar as the shaft flexes is responsible for many shaft failures in service. A limited

amount of fatigue test data has been generated for steel shafts with press-fitted, plain (without grooves or tapers) collars in pure bending. These data, from several sources, show typical fatigue life reductions to range from about 50 to 70 percent (ref. 5). Therefore the approximate range of press-fitted collar factors is

$$k_f = 0.3 \text{ to } 0.5$$

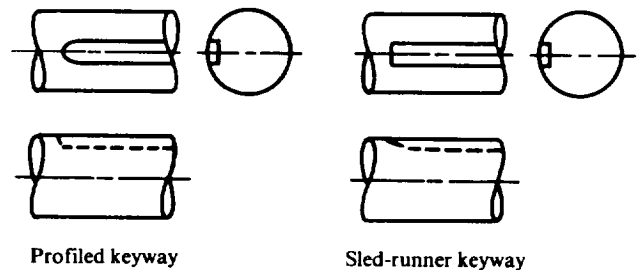
Larger shafts, with diameters greater than about 7.6 cm (3 in.), tend to have k_f values less than 0.4 when the collars are loaded. Smaller shafts with unloaded collars tend to have k_f values greater than 0.4. The effect of interference pressure between collar and shaft over a wide range has been found to be small, except for very light fits (less than about 28 MPa, or 4000 psi), which reduce the penalty to fatigue strength (ref. 5). Surface treatments that produce favorable compressive residual stresses and hardening, such as cold rolling, peening, induction, or flame hardening, can often fully restore fatigue strength ($k_f = 1$) (ref. 7). Stepping the shaft seat with a generous shoulder fillet radius or providing stress-relieving grooves on the bore of the collar can also substantially improve strength.

Residual Stress Factor k_g

The introduction of residual stress through various mechanical or thermal processes can have significant harmful or beneficial effects on fatigue strength. Residual stresses have the same effect on fatigue strength

TABLE V.—FATIGUE STRESS CONCENTRATION FACTORS—TYPICAL VALUES FOR KEYWAYS IN SOLID, ROUND STEEL SHAFTS

[From ref. 15; nominal stresses should be based on section modulus for total shaft section.]



Steel	Profiled keyway		Sled-runner keyway	
	Bending	Torsion	Bending	Torsion
	Fatigue stress concentration factors, $(k_e)_b$ and $(k_e)_t$			
Annealed (<200 BHN)	0.63	0.77	0.77	0.77
Quenched and drawn (>200 BHN)	.50	.63	.63	.63

as mean stresses of the same kind and magnitude. Thus residual tensile stresses behave as static tensile loads, which reduce fatigue strength, while residual compressive stresses behave as static compressive stresses, which increase fatigue strength. Table VI lists the most common manufacturing processes and the type of residual stress they are likely to produce. The extent that the residual tensile stresses from these processes reduce or benefit fatigue strength depends on several factors, including the severity of the loading cycle and the yield strength of the material in question. Since the maximum residual stress (either compressive or tensile) that can be produced in a part can be no greater than the yield strength of the material minus the applied stress, harder, higher strength materials can benefit more or be harmed more by residual stress (ref. 16). This, coupled with an increase in notch sensitivity, makes it important to stress relieve welded parts made from stronger steels and increases the need to cold work critical areas. For low-cycle-fatigue applications it usually does not pay to shot peen or cold roll mild steel parts with relatively low yield strengths since much of the beneficial residual compressive stress can be "washed out" with the first application of a large stress.

Cold working of parts or the other means listed in table VI to instill residual compressive stress are most often applied to minimize or eliminate the damaging effect of a notch, a fillet, or other defects producing high stress concentrations or residual tensile stresses. Cold-working processes not only generate favorable compressive stresses, but also work hardens the surface of the part and thus increase fatigue strength. The following discussion reviews some of the processes that generate residual stresses and their likely effect on fatigue.

Prestressing.—Prestressing is commonly employed in the manufacture of springs and torsion bars to produce a surface with high residual compressive stress. When

applied to notched steel tensile specimens having K_t values of 2.5 and 3.2, pretest stretching completely eliminates the notch effect (ref. 16). Stretching causes the notch to yield locally in tension. When the stretching load is released, the "spring back" from the surrounding, unyielded material creates large residual compressive stresses in the notch region.

Shot peening.—Shot peening is also used in the manufacture of springs and for shafts that have been plated, welded, or cold straightened. Normally, peening is only required at the point of stress concentration. Keyways, splines, fillets, grooves, holes, etc., can be successfully treated. Peening is also useful in minimizing the adverse effects of corrosion fatigue and fretting fatigue. It is effective in restoring the fatigue strength of rough forged shafts with decarburized surfaces and those that have been heavily machined or ground. Gentle grinding or lapping operations after peening for improved surface finish will have little detrimental effect as long as the layer removed is less than about 10 percent of the induced compressive layer (ref. 7). Generally speaking, if the depth and magnitude of the compressive stress are sufficiently great, the peening process can virtually negate the effect of a notch or other stress concentration. Accordingly, k_g is approximately $0.5/k_a k_e$ to $1/k_a k_e$ depending on the application. References 7, 16, and 17 should be consulted for more detail.

Surface rolling.—Surface rolling can be even more effective than shot peening, since it can produce a larger and deeper layer of compressive stress and also achieve a higher degree of work hardening. Furthermore the surface finish remains undimpled. With heavy cold rolling the fatigue strength of even an unnotched shaft can be improved up to 80 percent according to test data appearing in reference 7. However, like peening, cold rolling is normally applied at points of high stress concentration and where residual tensile stresses are present. Surface rolling of railroad wheel axles and crank pins is commonplace. The fatigue strength of crankshafts has been shown to increase by 60 to 80 percent when the fillets are rolled with steel balls (ref. 7).

Hardening processes.—Hardening processes such as flame and induction hardening as well as case carburizing and nitriding can considerably strengthen both unnotched and notched parts. This arises from the generation of large residual compressive stresses in combination with an intrinsically stronger, hardened surface layer. Rapid quenching tends to increase both of these strengthening effects. A helpful rule to remember is that the first layer of material to cool is in compression while the last to cool is in tension. These hardening techniques are particularly effective in combating corrosion fatigue and fretting fatigue. Flame hardening of notched and unnotched carbon steel rotating beam specimens typically increases fatigue strength from 40 to 190 percent; axles with diameters from 50 to 240 mm (2 to

TABLE VI.—MANUFACTURING PROCESSES THAT PRODUCE RESIDUAL STRESSES

Beneficial residual compressive stress	Harmful residual tensile stress
Process	
Prestressing or overstraining Shot or hammer peening Sand or grit blasting Cold surface rolling Coining Tumbling Burnishing Flame or induction hardening Carburizing or nitriding	Cold straightening Grinding or machining Electrodischarge machining (EDM) Welding Flame cutting Chromium, nickel, or zinc plating

9.5 in.) and press-fitted wheels show 46 to 246 percent improvement (ref. 7). Induction hardening of unnotched carbon and alloy steel specimens shows fatigue strength improvements from 19 to 54 percent (ref. 7). Case carburizing of plain rotating-beam specimens made from various steels causes a 32 to 105 percent increase in fatigue strength; notched specimens (0.5-mm-radius notch) show a strength improvement of 82 to 230 percent (ref. 7). Similarly, plain nitrided specimens experience a 10 to 36 percent benefit and notched nitrided specimens improve 50 to 300 percent (ref. 7).

Cold straightening.—The presence of residual tensile stresses due to the processes listed in table VI requires a derating in fatigue strength. Cold-straightening operations tend to introduce tensile residual stress in areas where the material was originally overstrained in compression. References 7 and 15 report fatigue strength reductions of 20 to 50 percent as a result of cold straightening and state that such reductions can be avoided if hammer peening or shot peening is applied during straightening. Overstraightening and bending back is also helpful.

Nickel and chromium plating.—Although nickel and chromium plating are effective in increasing wear resistance and in improving resistance to corrosion or corrosion fatigue, the resulting residual tensile stresses generated in the plated layer can cause up to a 60 percent reduction in the fatigue limits according to published data (ref. 7). Much of the loss in fatigue strength can be restored if nitriding, shot peening, or surface rolling is performed before plating. Shot peening after plating may be even more effective.

Corrosion Fatigue Factor k_f

The formation of pits and crevices on the surface of shafts due to corrosion, particularly under stress, can cause a major loss in fatigue strength. Exposed shafts on outdoor and marine equipment as well as those in contact with corrosive chemicals are particularly vulnerable. Corrosion fatigue cracks can even be generated in stainless steel parts where there may be no visible signs of rusting. Furthermore designs strictly based on the fatigue limit may be inadequate for lives much beyond 10^6 or 10^7 cycles in a corrosive environment. Metals that are fatigue tested even in a mildly corrosive liquid like freshwater rarely show a distinct fatigue limit (ref. 7). For example, the S-N curve for mild carbon steel tested in a saltwater spray shows a very steep downward slope, even beyond 10^8 cycles. Corrosion fatigue strength has also been found to decrease with an increase in the rate of cycling. Thus both the cycling rate and the number of stress cycles should be specified when quoting fatigue strengths of metals in a corrosive environment. Reference 7 contains a wealth of information on the corrosive fatigue strength of metals. Typically, the bending fatigue strengths of

chromium steels at 10^7 cycles when tested in a saltwater spray range from about 60 to 80 percent of the air-tested fatigue limit. In freshwater the fatigue limits of carbon and low-alloy steels are approximately 80 percent of the air limit for 275-MPa (40-ksi) tensile strength steels, 40 percent for 550-MPa (80-ksi) steels, and 20 percent for 1240-MPa (180-ksi) steels when cycled in bending at 1450 cycles/min for 2×10^7 cycles (ref. 7). In saltwater under the same test conditions the fatigue limits of carbon steels are about 50 percent, 30 percent, and 15 percent of the air limit for steels having σ_u of 275, 550, and 1240 MPa (40, 80, and 180 ksi), respectively. Surface treatments such as galvanizing, sherardizing, zinc or cadmium plating, surface rolling, or nitriding can normally restore the fatigue strength of carbon steels tested in freshwater or saltwater spray to approximately 60 to 90 percent of the normal fatigue limit in air (ref. 7).

Miscellaneous Effects Factor k_j

Since fatigue failures nearly always occur at or near the surface of the shaft, where the stresses are the greatest, surface condition strongly influences fatigue life. A number of factors that have not been previously discussed but are known to affect the fatigue strength of a part are

- (1) Fretting corrosion
- (2) Thermal cycle fatigue
- (3) Electrochemical environment
- (4) Radiation
- (5) Shock or vibration loading
- (6) Ultra-high-speed cycling
- (7) Welding
- (8) Surface decarburization

Although only limited quantitative data have been published for these factors (refs. 7, 8, and 16), they should, nonetheless, be considered and accounted for if applicable. Some of these factors can have a considerable effect on the shaft's endurance characteristics. In the absence of published data, it is advisable to conduct fatigue tests that closely simulate the shaft condition and its operating environment.

Variable-Amplitude Loading

The analysis presented thus far assumes, for simplicity, that the nominal loads acting on the shaft are essentially of constant amplitude and that the shaft life will exceed 10^6 or 10^7 cycles. However, most shafts in service are generally exposed to a spectrum of loading. Occasionally shafts are designed for lives that are less than 10^6 cycles for purposes of economy. Both of these requirements complicate the method of analysis and increase the uncertainty of the prediction. Under these conditions,

prototype component fatigue testing under simulated loading becomes even more important.

Short-Life Design

Local yielding of notches, fillets, and other points of stress concentration is to be expected for shafts designed for short service lives (less than about 1000 cycles). Since fatigue cracks inevitably originate at these discontinuities, the plastic fatigue behavior of the material dictates its service life. Most materials have been observed to either cyclicly harden or soften, depending on their initial state, when subjected to cyclic plastic strain. Therefore the cyclic fatigue properties of a material, which can be significantly different from its static or monotonic strength properties, need to be considered in the analysis. For short, low-cycle-life designs the plastic notch strain analysis, discussed in detail in references 16, 18, and 19, is considered to be the most accurate design approach. This method, used widely in the automotive industry, predicts the time to crack formation from an experimentally determined relationship between local plastic and elastic strain and the number of reversals to failure. The aforementioned references should be consulted for details of this method.

Intermediate- and Long-Life Designs

For intermediate- and long-life designs both total strain-life and nominal stress-life (S-N curve) methods have been successfully applied. Although the nominal stress-life approach, adopted herein, is much older and more widely known, both methods have provided reasonable fatigue life predictions and should be applied to the same problem for comparison whenever possible. However, only the nominal stress-life method is outlined herein.

Obviously the key to accurate fatigue life prediction is obtaining a good definition of the stress-life (S-N) characteristics of the shaft material. Mean bending or torsional stress effects should be taken into account if present. Furthermore a good definition of the loading history is also required. Even when these requirements are met, the accuracy of the prediction is approximate with today's state of knowledge. As an example, an extensive cumulative fatigue damage test program was conducted by the Society of Automotive Engineers to assess the validity of various fatigue life prediction methods (ref. 18). Numerous simple-geometry, notched steel plate specimens were fatigue tested in uniaxial tension. Tests were conducted under constant-amplitude loading and also under a variable-amplitude loading that closely simulated the service loading history. The test specimens' material fatigue properties and the actual force-time history were very well defined. Under these well-controlled conditions, predicted mean life from the best available method was within a factor of 3 (1/3 to 3

times) of the true experimental value for about 80 percent of the test specimens; some of the other methods were considerably less accurate (ref. 18). Under less ideal conditions, such as when the loading history and material properties are not as well known or when a multiaxial stress state is imposed, a predictive accuracy within a factor of 10 of the true fatigue life would not be unacceptable with today's state of knowledge.

The following is a greatly simplified approach to estimating the required shaft diameter for a limited number of stress cycles under a variable-amplitude loading history. It assumes that the loading history can be broken into blocks of constant-amplitude loading and that the sum of the resulting fatigue damage at each block loading equals 1 at the time of failure in accordance with the Palmgren-Miner linear damage rule. Great care must be exercised in reducing a complex, irregular loading history to a series of constant-amplitude events in order to preserve the fidelity of the prediction. Reference 18 discusses the merits of several cycle counting schemes that are commonly used in practice for prediction purposes.

A shortcoming of Miner's rule is that it assumes that damage occurs at a linear rate without regard to the sequence of loading. There is ample experimental evidence that a virgin material will have shorter fatigue life when first exposed to high cyclic stress and then low cyclic stress; that is, Miner's sum is less than 1 (refs. 7 and 19). This "overstressing" is thought to create sub-microscopic cracks in the material structure that can accelerate the damage rate. On the other hand, test specimens exposed first to stresses just below the fatigue limit are often stronger in fatigue than when new. This "coaxing" or "understraining" effect, which can produce Miner's sums much larger than 1, is believed to be due to a beneficial strain-aging phenomenon. Although Miner's sums at the time of failure can range from 0.25 to 4 depending on loading sequence and magnitude, the experimental range shrinks to approximately 0.6 to 1.6 when the loading is more random (ref. 19). This is often acceptable for failure estimates. More complicated cumulative damage theories have been devised to account for "sequencing" effects (in fact ref. 19 discusses seven different ones), but none of them have been shown to be completely reliable for all practical shaft-loading histories. In most cases, Miner's rule serves almost as well and because of its simplicity it is still preferred by many.

To determine the proper shaft size for a given number of stress cycles under a variable-amplitude loading situation, it is necessary to construct an S-N curve for the shaft under the proper mean loading condition. If an experimentally determined S-N curve for the shaft material is available, of course, it is to be used after being corrected for the fatigue life modifying factors identified in equation (19). However, if actual test data are not available, it is still possible to generate a reasonable

estimate of the S-N characteristics, as shown in figure 6. Although several methods have been proposed for mathematically constructing an S-N diagram (refs. 7, 8, and 19), the method adopted herein is similar to that recommended by the Society of Automotive Engineers (ref. 20). In figure 6 a straight line connects the fatigue strength coefficient σ'_f at 1 cycle with the shaft's corrected fatigue limit σ_f at 10^6 stress cycles (or 10^7 cycles if applicable) on log-log coordinates. The coefficient σ'_f is essentially the true stress (considering necking) required to cause fracture on the first applied bending stress cycle. It is normally greater than the nominal tensile strength of the material σ_u . This method assumes that the fracture strength of the material in the outer fibers of the shaft is unaffected by the presence of mean bending, torsional stresses, or a notch. Any initial mean or residual stress in the outer fibers will be lost by local yielding upon first application of the high bending or torque load. For axial loading this assumption is not correct since the whole section rather than the outer fibers must support the mean load (ref. 16). Typical values of σ'_f for a number of different steel compositions along with other strength properties are given in table II (refs. 21 and 22). For steels in the low and intermediate hardness range (less than 500 BHN) not listed in table II (ref. 20), a rough approximation is

$$\left. \begin{aligned} \sigma'_f &\approx \sigma_u + 345 \text{ MPa} \\ \text{or} \\ \sigma'_f &\approx \sigma_u + 50\,000 \text{ psi} \end{aligned} \right\} \quad (27)$$

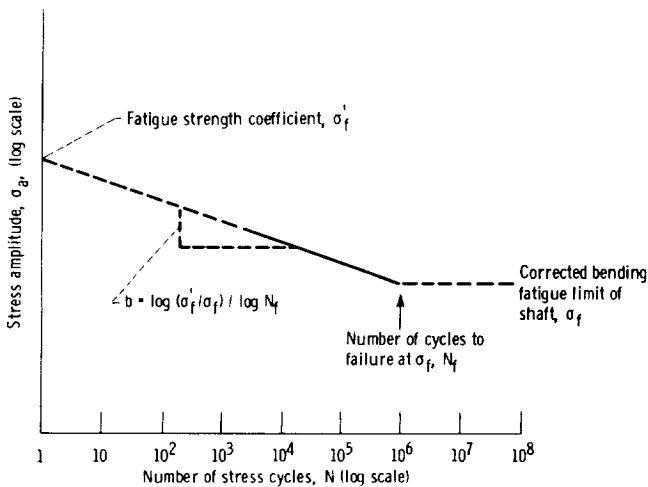


Figure 6.—Generalized stress-life curve constructed from corrected bending fatigue limit of shaft σ_f and fatigue strength coefficient σ'_f .

where σ_u is the ultimate tensile strength. From this simple approximation and that given in equation (20), a reasonably good correlation can be obtained with reversed bending fatigue data for different strength steels (ref. 23), as shown in figure 7.

The fatigue limit of the shaft σ_f can be found from the fatigue limit of a polished, unnotched specimen σ'_f corrected by the k factors of equation (19). This method is compared with both notched and unnotched fatigue data from reference 24 in figure 8. From the geometry of the notch and the steel's tensile strength, the values $K_f=1.76$, $q=0.79$, and $k_f=0.63$ can be found. Note from this figure how shot peening, in this case, virtually eliminates the detrimental notch effect. If a mean bending moment M_m or mean torsional load T_m is present, the specimen fatigue life σ'_f is approximately altered according to equation (18) as follows:

$$\sigma'_{f,m} = \sigma'_f \left\{ \left[1 - 77.8 \left(\frac{T_m}{d^3 \sigma_y} \right)^2 \right]^{1/2} - 10.2 \left(\frac{M_m}{d^3 \sigma_u} \right) \right\} \quad (28)$$

where $\sigma'_{f,m}$ is the test specimen fatigue limit with $M_m \neq 0$ or $T_m \neq 0$.

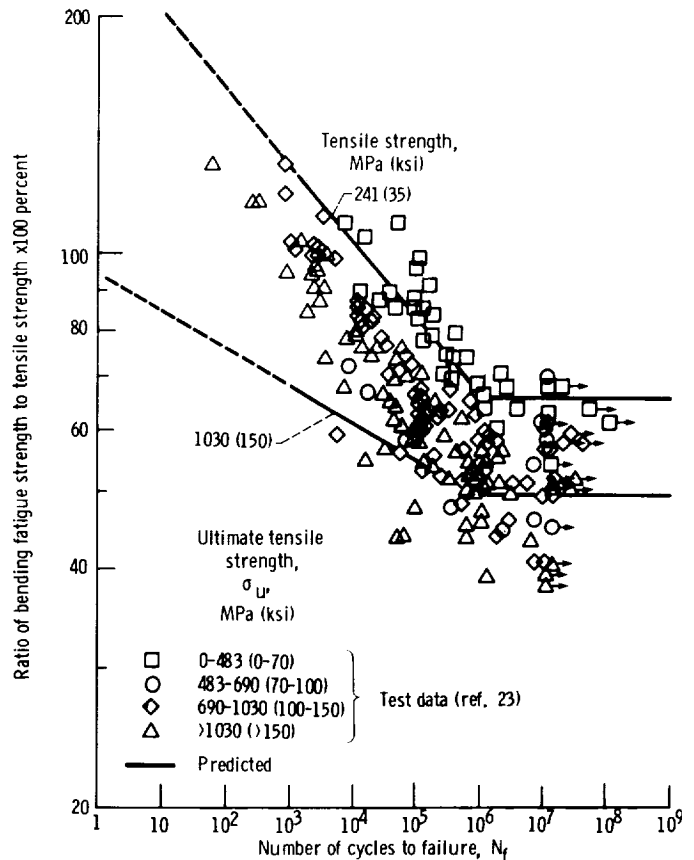


Figure 7.—Stress-life characteristics as a function of predicted and measured tensile strengths of steels in reversed bending. (Test data from ref. 23.)

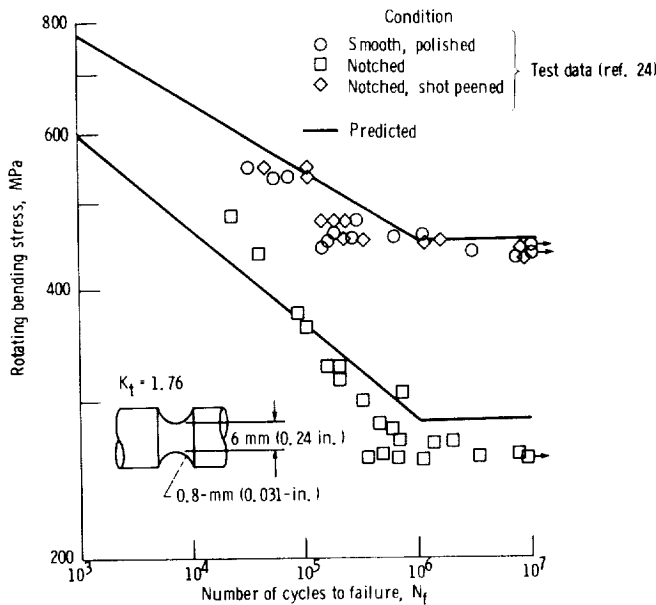


Figure 8.—Predicted and experimental stress-life characteristics of smooth, notched and shot-peened steel rotating-beam specimens. Ultimate tensile strength, σ_u , 897 MPa. (Test data from ref. 24.)

Assume that the shaft is exposed to a series of alternating bending moments of constant amplitude M_{a1} for n_1 loading cycles, M_{a2} for n_2 cycles, M_{a3} for n_3 cycles, etc. Then according to Miner's rule

$$\frac{n_1}{N_1} + \frac{n_2}{N_2} + \frac{n_3}{N_3} = 1 \quad (29)$$

where N_1 is the number of cycles to failure at bending moment M_{a1} , N_2 is the cycles to failure at M_{a2} , etc.

From the straight line on the log-log S-N plot of figure 6, it is clear that

$$\frac{\sigma_{a1}}{\sigma_f} = \left(\frac{N_f}{N_1}\right)^b, \quad \frac{\sigma_{a2}}{\sigma_f} = \left(\frac{N_f}{N_2}\right)^b, \quad \frac{\sigma_{a3}}{\sigma_f} = \left(\frac{N_f}{N_3}\right)^b \quad (30)$$

where σ_{a_i} is the alternating bending stress at bending moment M_{a_i} , N_f is the number of stress cycles corresponding to the fatigue limit σ_f (usually 10^6 to 10^7 cycles), and b is the slope of the S-N curve taken as a positive value where $b = \log(\sigma_f'/\sigma_f)/6$ for $N_f = 10^6$ cycles or $b = \log(\sigma_f'/\sigma_f)/7$ for $N_f = 10^7$ cycles. Substituting equation (30) back into equation (29), noting $\sigma_{a_i} = 32 M_{a_i}/\pi d^3$, and simplifying yield

$$d^3 = \frac{32(\text{FS})}{\pi\sigma_f} \left[\frac{n_1}{N_f} (M_{a1})^{1/b} + \frac{n_2}{N_f} (M_{a2})^{1/b} + \frac{n_3}{N_f} (M_{a3})^{1/b} \right]^b \quad (31)$$

where the factor of safety term FS has been introduced.

Note that since σ_f and hence b can depend on the shaft diameter d through equations (19) and (28), it may be necessary to take an initial guess of d to calculate σ_f and b so that a d from equation (31) can be found. The most recently found d should be used to update σ_f and the calculation repeated until the change in d becomes acceptably small. (A good starting point is to calculate d from equation (31) by assuming that no mean load is present.)

Application Example

To illustrate application of this method, consider that a shaft is to be designed with an FS of 2 from quenched and tempered SAE 1045 steel (225 BHN, $\sigma = 724$ MPa, and $\sigma_y = 634$ MPa from table II) for 100 000 cycles under a steady torque of 3000 N-m and the variable-bending-moment schedule in table VII.

The fatigue limit of a smooth 1045 steel specimen without mean stress σ_f^* is listed as 323 MPa at $N_f = 10^6$ cycles in table II. (This is somewhat smaller than the approximation $0.5 \sigma_u$, or 362 MPa.)

Starting with an initial shaft diameter guess of $d = 0.055$ m, the effect of the mean torque of 3000 N-m on σ_f^* can be found from equation (28) as follows:

$$\begin{aligned} \sigma_{f,m}^* &= 323 \times 10^6 \left[1 - 77.8 \left(\frac{3000}{0.055^3 \times 634 \times 10^6} \right)^2 \right]^{1/2} \\ &= 313 \text{ MPa} \end{aligned}$$

If we assume that in this example the product of all of the k factors described by equation (19) is equal to 0.4, the shaft's corrected bending fatigue limit is

$$\sigma_f = 0.4 (313 \times 10^6) = 125 \text{ MPa}$$

For this material σ_f' is given as 1227 MPa, so the S-N curve slope is

TABLE VII.—VARIABLE-BENDING-MOMENT SCHEDULE

Alternating bending moment, M_{a_i} , N-m	Time, percent	Number of loading cycles, n_i	Fraction of number of cycles of failure at corrected bending fatigue limit, n_i/N_f
2000	15	15 000	0.015
1500	35	35 000	.035
1000	50	50 000	.050
	100	100 000	

$$b = \log(1227/125)/6 = 0.165$$

or

$$1/b = 6.05$$

Finally, for an FS = 2.0, the required shaft diameter d can be found from equation (31) to be

$$d^3 = \frac{32(2.0)}{\pi(125 \times 10^6)} [0.015 (2000)^{6.05} + 0.035(1500)^{6.05} + 0.05(1000)^{6.05}]^{0.165}$$

$$= 1.71 \times 10^{-4} \text{m}^3$$

or

$$d = 0.056 \text{ m}$$

(This diameter is sufficiently close to the initial guess that a repeat calculation is not required.) It is instructive to note that if the calculation were repeated considering that only the maximum bending moment of 2000 N-m acted 15 percent of the time and that the shaft ran unloaded the rest of the time, that is

$$M_{a2} = M_{a3} = 0$$

then

$$d = 0.054 \text{ m}$$

The insignificant reduction in shaft diameter from ignoring the lower loads clearly illustrates the dominant effect that peak loads have on fatigue life. This is also apparent from figure 6, where life is inversely proportional to the $1/b$ power of stress amplitude. The exponent $1/b$ typically ranges from about 5 for heavily notched shafts to about 14 for some polished, unnotched steel test specimens without mean stresses (table II). Even at a modest $1/b$ value of 6, 64 times more fatigue damage is caused by doubling the alternating bending moment or bending stress amplitude. This underscores the necessity of paying close attention to overload conditions in both shaft and structural element fatigue designs.

Rigidity

Gears, bearings, couplings, and other drivetrain components perform best when they are maintained in correct alignment. Operating positioning errors due to shaft, bearing, and housing deflections under load can

lead to higher operating temperatures and vibratory loads as well as shorter service life. Shaft stiffness rather than strength can sometimes dictate shaft size, particularly for high-speed, precision machinery, where accurate alignment becomes more critical. Dynamic rather than static deflections and runouts determine operating characteristics, so shaft vibration should also be considered.

The permissible values of shaft deflection are normally dictated by the sensitivity of the selected transmission component to positional errors and the quality of service desired. For example, small, high-speed, precision gears will obviously require greater positioning accuracy than large, low-speed gears intended for normal industrial service. Thus it is good practice to determine the effects of shaft deflection on the performance of the specific component rather than to use generalized "rules of thumb." However, certain general rules can often be helpful for preliminary design purposes.

For gears, positional errors due to shaft, bearing, and housing deflections cause changes in the operating center distance, backlash, and a maldistribution of tooth loads that lowers gear mesh capacity. Involute gears can normally tolerate somewhat greater changes in operating center distance, that is, parallel deflections between driver and driven gearshafts, than changes in parallelism (misalignment) between shafts. According to reference 25, the deviation between the operating and ideal center distances of involute toothed gears for proper meshing action should be less than either 2 percent of the center distance or one-quarter of the working depth, whichever is smaller. For spur and straight bevel gears the working depth equals twice the ratio of pitch diameter to number of teeth. Permissible misalignment values for gears can be more restrictive depending on the quality of service desired, according to table VIII (adapted from ref. 26). For bevel gears with diameters of 152 to 381 mm (6 to 15 in.), some manufacturers recommend that neither pinion nor gear deflections generally exceed 0.076 mm (0.003 in.). These are general maximum limits that can usually be improved on by mounting gears close to bearings and

TABLE VIII.—REPRESENTATIVE
MAXIMUM PERMISSIBLE
MISALIGNMENT VALUES FOR
GEARED SHAFTS

[From ref. 26]

Gear train quality	Misalignment of shaft length between bearings, rad (in./in.)
Commercial	0.005
Precision	.003
High precision	.0015
Ultra precision	.001

using a straddle mount rather than an overhung mount when possible.

Shaft misalignment through plain and rolling-element bearings can lead to shorter life by causing stress concentrations to develop. For journal bearings the shaft angle through the bearing should never cause contact between the shaft and the bearing. Thus the shaft angle in radians should never exceed the ratio of bearing diametral clearance to bearing width. Spherical and deep-grooved ball bearings have greater tolerance to misalignment than cylindrical and tapered roller bearings according to table IX (adapted from ref. 27).

Flexible shaft couplings are designed to accept some degree of shaft misalignment and offset. Acceptable limits are normally established for gear couplings by maximum permissible sliding velocities and for foil and diaphragm couplings by flexible-element fatigue. Coupling manufacturers' product literature should be consulted for recommended values.

In some applications where there is a need to synchronize the position of several machine elements mounted on the same shaft, the maximum angular deflection of the shaft between elements may need to be limited. Permissible values for shaft twist commonly quoted in the literature are 1° twist for a shaft length of 20 diameters or 3.05 m (10 ft), whichever is more stringent. For a solid circular shaft in torsion the shaft twist θ in degrees due to torque T is given by

$$\theta = \frac{584TL}{d^4G} \quad (32)$$

where

d shaft diameter

G elastic shear modulus (79.3 GPa, or 11.5×10^6 psi, for steel)

L shaft length of circular shaft or equivalent length for noncircular shaft from table I

TABLE IX.—LIMITS OF ROLLING-ELEMENT BEARING MISALIGNMENT BASED ON MANUFACTURER'S GENERAL EXPERIENCE

[From ref. 27.]

Bearing type	Allowable misalignment, rad (in./in.)
Cylindrical and tapered roller	0.001
Spherical	0.0087
Deep-grooved ball	0.0035-0.0047

Shaft Materials

Power-transmitting shafts and axles are most commonly machined from plain carbon (AISI/SAE 1040, 1045, and 1050) or alloy (AISI/SAE 4140, 4145, 4150, 4340, and 8620) steel bar stock. The bar stock may be either hot rolled or cold finished (cold drawn and machined). Cold drawing improves not only mechanical strength but also machinability, surface finish, and dimensional accuracy. Hot-rolled shafts are often quenched and tempered for greater strength and then finished (turned and polished or turned, ground, and polished) for improved finish and dimensional accuracy. Table X shows normal surface finish ranges (ref. 28). Table XI shows typical manufacturing tolerances (ref. 29).

In general, standard commercial line shafting up to 76 mm (3 in.) in diameter is normally cold drawn and is sufficiently straight that no turning is normally needed. However, a straightening operation is usually required if keyways are cut into a shaft that has not been subsequently stress relieved, since the keyways relieve the compression on the shaft surface generated during cold drawing. However, turned bars can be machined or key seated with practically no danger of warpage. The diameter of machinery shafting is normally available in 1/16-in. increments from 1/2 to 2 1/2 in., in 1/8-in. increments to 4 in., and in 1/4-in. increments to 5 in. with standard stock lengths of 16, 20, and 24 ft. Transmission shafting diameters are graduated in 1/4-in. increments from 15/16 to 27/16 in. and 1/2-in. increments to 5 15/16 in. (Standard transmission shafting in bar stock is normally available only in inch sizes in the United States.)

Crankshafts and hollow, large-diameter, or flanged shafts are often forged or partially forged and then ground or machined to final dimensions. Quite often,

TABLE X.—NORMAL RANGE OF SURFACE FINISH FOR SHAFT FINISHING OPERATIONS

[From ref. 28. Surface finish of commercial-quality steel bars normally supplied at lower limit of each range.]

Finishing operation	Normal range of surface finish (AA) ^a	
	μm	$\mu\text{in.}$
Cold drawing	1.27-3.18	50-125
Turning and polishing	0.38-1.02	15-40
Cold drawing, grinding, and polishing	0.20-0.51	8-20
Turning, grinding, and polishing	0.20-0.51	8-20

^aAA denotes arithmetic average surface roughness. Root-mean-square (rms) roughness = 1.1 x AA roughness.

TABLE XI.—TYPICAL MANUFACTURING TOLERANCES OF COLD-FINISHED CARBON STEEL ROUND BARS

[From ref. 29.]

Diameter range		Cold drawn or turned and polished				Ground and polished			
mm	in.	Carbon content, percent				Turned		Cold drawn	
		≤ 0.28		0.28–0.55					
		Tolerance ^a		Tolerance ^a		Tolerance ^a		Tolerance ^a	
		mm	in.	mm	in.	mm	in.	mm	in.
To 38.1	To 1.5	0.051	0.002	0.076	0.003	0.025	0.001	0.025	0.001
>38.1–63.5	>1.5–2.5	.076	.003	.102	.004	.038	.0015	.038	.0015
>63.5–76.2	>2.5–3	----	----	----	----	.051	.002	.051	.002
>63.5–101.6	>2.5–4	.102	.004	.127	.005	----	----	----	----
>76.2–101.6	>3–4	----	----	----	----	.076	.003	.076	.003
>101.6–152.4	>4–6	.127	.005	.152	.006	.102	.004	----	----
>152.4	>6	----	----	----	----	.127	.005	----	----
>152.4–203.2	>6–8	.152	.006	.178	.007	----	----	----	----
>203.2–228.6	>8–9	.178	.007	.203	.008	----	----	----	----
>228.6	>9	.203	.008	.229	.009	----	----	----	----

^aAll tolerances are minus (undersized diameters).

crankshafts, forged shafts, and shafts of large cross section require a higher carbon steel or alloy steel to preserve strength. Steel grades 1046, 1052, 1078, 4340, and 5145 have been successfully used for crankshafts.

For some light-duty applications, low-strength, plain carbon steels such as 1018 and 1022 can be used. However, the cost saving expected by switching to a lower grade of steel can sometimes be negated by the need to increase the size of the shaft and the components attached to it. In many cases, particularly weight- and size-sensitive applications, it may be more cost effective to switch to a higher-strength alloy steel such as 4140 or 4340.

Case-carburized steels such as 8620, 1060, and the 4000 series are frequently used for splined and geared shafts. Case-hardened shafts are also specified for bearing applications where the balls or rollers contact the shaft directly. General design information on shafting steels can be found in reference 14.

Because both low- and high-strength steels have essentially equal elastic modulus properties, it is pointless to specify a more expensive, higher strength steel for applications where shaft rigidity is the deciding factor. Only an increase in shaft cross section or a decrease in the bearing support span can lessen the shaft deflection under a fixed load.

Shaft Vibration

As the speed of a rotating shaft is increased, a critical speed (system natural frequency) may be approached that

can significantly increase shaft deflections and vibrations. Operation at or near a system critical speed can lead to high vibration amplitudes that, if left unchecked, can substantially damage the machine. The subject of rotor dynamics is much too diverse (e.g., refs. 30 to 37) to be covered here in detail. Therefore the following discussion is limited to some of the more basic design considerations with reference to more sophisticated approaches.

The avoidance of potentially dangerous vibrations through careful modeling of the shaft-bearing system should be undertaken early in the design process. Although a shaft may be sufficiently strong to meet service life requirements, it may not be sufficiently stiff (or soft) to avoid rotordynamics problems. Modern high-speed rotating machinery can be designed to operate at speeds substantially greater than the fundamental critical frequency (so-called supercritical shafting), but proper attention to balancing and provisions for damping are usually required (ref. 30). However, most rotating machinery is designed to operate at speeds below the first critical, and only this is addressed herein.

As a first approximation, the first critical or fundamental frequency of a shaft-bearing system with concentrated body masses can be found from the Rayleigh-Ritz equation (ref. 31) as follows:

$$\omega_c = \left(\frac{g \sum_1^m W_i \delta_i}{\sum_1^m W_i \delta_i^2} \right)^{1/2} \quad (33)$$

where

- g gravitational constant, 9.8 m/s² (386 in/s²)
 m total number of bodies
 ω_c first critical frequency, rad/s
 W_i weight of i th body
 δ_i static deflection of i th body

It should be emphasized that the proper deflections to use in equation (33) are those due to the weight of the body (gear, sprocket, etc.) and not those due to any external forces.

Equation (33) considers the shaft to be weightless; however, the shaft's weight can also be taken into account by dividing the shaft into a number of discrete elements. Then the weight of each shaft element acting at its center of gravity and its deflection can be readily included into the summation of equation (33). This technique can also be used to estimate the first natural frequency of the shaft by itself.

In applying equation (33) a judgment must be made as to whether the bearings will freely accommodate shaft misalignment (simply supported shaft) or resist misalignment (fixed support) or lie somewhere in between. Clearly shafts supported by spherical or self-aligning bearings can be treated as simply supported, and those supported by cylindrical or tapered roller bearings can normally be considered fixed. Furthermore bearings tend to behave more like a fixed support when supporting long, flexible shafts than when supporting short, rigid shafts, which have relatively small misalignment. When in doubt, the best course to follow is to calculate shaft deflections both ways to "bracket" the critical speed estimate.

Up until now the support bearings have been considered as laterally rigid. However, rolling-element and fluid-film bearings are not infinitely stiff and will contribute to shaft deflections. The effect of bearing lateral flexibility on the shaft system's critical speed can be approximately accounted for by calculating the additional deflection at each load point $\delta_{b,i}$ due to support bearing deflection. The total deflection at each load point δ_i to be incorporated into equation (33) will then equal the sum of that due to static shaft bending $\delta_{s,i}$ plus $\delta_{b,i}$, or $\delta_i = \delta_{s,i} + \delta_{b,i}$.

It is clear from equation (33) that the addition of bearing deflection reduces the critical speed relative to that for a shaft supported on completely rigid bearings. Normally this reduction in speed is relatively small (less than about 20 percent) since the support bearings and housing are usually significantly stiffer than the shaft. It also follows that the critical speed can be raised by reducing total shaft deflections such as by selecting stiffer bearings, preloading them, reducing support bearing span, increasing local shaft section diameter, or reducing transmission component weight.

This method is approximate in that it ignores inertia effects, assumes that bearings have linear deflection characteristics, and neglects damping and unbalance forces. If the predicted critical speed is within about 20 percent of the operating speed, it is desirable to perform a more detailed analysis. General critical-speed computer codes for shafts (refs. 33 and 34) can be used in place of or in addition to equation (33). Reference 32 is a comprehensive document that treats these topics and many others from a practical design standpoint. Hysteretic effects due to press-fitted components and splines, damping effects due to fluid-film bearings, gyroscopic effects due to turbine and compressor disks, and balancing methods are some of the other topics addressed. Multiplane balancing techniques are extremely important for minimizing shaft excursions for high-speed, flexible rotors. Reference 32 lists names and sources of a number of rotordynamics codes. Reference 34 includes a general critical-speed computer program that calculates the critical speed and mode shapes for a multispan shaft with any combination of couplings and bearings up to nine. Reference 35 is a good source of information for ball and cylindrical roller bearing stiffness values to be used for input data to critical-speed and rotordynamics response computer codes. Reference 36 gives considerable practical information on torsional vibration problems. Reference 37 provides a modern treatment of general vibration problems with discussion on modal analysis and application.

National Aeronautics and Space Administration
Lewis Research Center
Cleveland, Ohio, February 15, 1984

References

1. Rotary Motion Flexible Shafts, Seventh ed., S. S. White Industrial Products, Div. of Pennwalt, New Jersey, 1977.
2. Liquid Rocket Engine Turbopump Shafts and Couplings. NASA SP-8101, 1972.
3. Sadowy, M.: Shafts, Couplings, Keys, etc. Mechanical Design and Systems Handbook, H. A. Rothbart, ed., McGraw-Hill Book Co., 1964, pp. 27-1 to 27-29.
4. Lowell, C. M.: "A Rational Approach to Crankshaft Design," ASME Paper 55-A-57, Nov. 1955.
5. Peterson, R. E.: Stress Concentration Factors, John Wiley, 1974.
6. Roark, R. J.; and Young, W. C.: Formulas for Stress and Strain, Fifth ed., McGraw-Hill, 1975.
7. Forrest, P. G.: Fatigue of Metals. Pergamon Press, 1962.
8. Juvinall, R. C.: Engineering Considerations of Stress, Strain, and Strength. McGraw-Hill, 1967.
9. Loewenthal, S. H.: Proposed Design Procedure for Transmission Shafting Under Fatigue Loading. NASA TM-78927, 1978.
10. Noll, G. C.; and Lipson, C.: Allowable Working Stresses. Proc. Soc. Exp. Stress Anal. vol. III, no. 2, 1946, pp. 86-109.

11. Kuguel, R.: A Relation Between Theoretical Stress Concentration Factor and Fatigue Notch Factor Deduced from the Concept of Highly Stressed Volume. Proc. Am. Soc. Test. Mater., vol. 61, 1969, pp. 732-748.
12. Horgler, O. J.; and Neifert, H. R.: "Fatigue Properties of Large Specimens with Related Size and Statistical Effects," Symposium on Fatigue with Emphasis on Statistical Approach, Special Technical Publication No. 137, ASTM, 1953.
13. Stulen, F. B.; Cummings, H. N.; and Schulte, W. C.: Preventing Fatigue Failures. Mach. Des., vol. 33, no. 9, June 22, 1961, pp. 159-165.
14. ASM Committee on Fatigue of Steel, The Selection of Steel for Fatigue Resistance Metals Handbook. Vol. 1, Properties and Selection of Metals, eighth ed., T. Lyman, ed., American Society for Metals, 1961, pp. 217-224.
15. Lipson, C.; Noll, G. C.; and Clock, L. S.: Stress and Strength of Manufactured Parts. McGraw-Hill, 1950.
16. Fuchs, H. O.; and Stephens, R. I.: Metal Fatigue in Engineering. John Wiley, 1980.
17. Almen, J. O.; and Black, P. H.: Residual Stresses and Fatigue in Metals. McGraw-Hill, 1963.
18. Wetzel, R. M., ed.: Fatigue Under Complex Loading: Analyses and Experiments. Advances in Engineering, vol. 6, Society of Automotive Engineers, 1977.
19. Collins, J. A.: Failure of Materials in Mechanical Design: Analysis. John Wiley, 1981.
20. Graham, J. A., ed.: Fatigue Design Handbook. Society of Automotive Engineers, Inc., 1968.
21. SAE Information Report; Technical Report on Fatigue Properties—SAE J1099, SAE Handbook, SAE, 1978, p. 4.44.
22. SAE Information Report; Estimated Mechanical Properties and Machinability of Hot Rolled and Cold Drawn Carbon Steel Bars—SAE J414, SAE Handbook, 1978, pp. 3.14-3.15.
23. Heywood, R. B.: Designing Against Fatigue of Metals. Reinhold, 1962, p. 30.
24. Harris, W. J.: Metallic Fatigue. Pergamon Press, 1961, p. 48.
25. Tuplin, W. A.; and Michalec, G. W.: Gearing Mechanical Design and Systems Handbook, H. A. Rothbart, ed., McGraw-Hill Book Co., 1964, pp. 32-18 to 32-19.
26. Michalec, G. W.: Precision Gearing: Theory and Practice, John Wiley, 1966, p. 346.
27. Bamberger, E. N.: Life Adjustment Factors for Ball and Roller Bearings—An Engineering Design Guide. American Society of Mechanical Engineers, 1971.
28. SAE Recommended Practice; High Strength Carbon and Alloy Die Drawn Steel. SAE J935, SAE Handbook, SAE, 1978, pp. 3.03-3.04.
29. Buyer's Guide to Cold Finished Steel Bars. Bulletin 15-1, Joseph T. Ryerson and Sons, Inc., 1975.
30. Gunter, E. J.: Dynamic Stability of Rotor-Bearing Systems. NASA SP-113, 1966.
31. Temple, G. A.; and Bickley, W. G.: "Rayleigh's Principle and Its Application to Engineering Problems," Dover Publications, New York, 1949.
32. Rieger, N. F.: Vibration of Rotating Machinery. Part 1: Rotor-Bearing Dynamics, Second ed. The Vibration Institute, 1982.
33. Pan, C. H. T.; Wu, E. R.; and Krauter, A. I.: Rotor-Bearing Dynamics Technology Design Guide. AFAPL-TR-78-6, Air Force Aero Propulsion Lab., Pt. 1-Flexible Rotor Dynamics, 1980 (AD-A087806); Pt. 2-Ball Bearings, 1978 (AD-A065554); Pt. 3-Tapered Roller Bearings, 1979 (AD-A074827); Pt. 4-Cylindrical Roller Bearings, 1979 (AD-A082355); Pt. 5-Dynamic Analysis of Incompressible Fluid Bearings, 1980 (AD-A085106); Pt. 6-Status of Gas Bearing Technology Applicable to Aero Propulsion Machinery, 1980 (AD-A094167); Pt. 8-A Computerized Data Retrieval System for Fluid Film Bearings, 1980 (AD-A094087); Pt. 9-User's Manual, 1981 (AD-A100210).
34. Trivisonno, R. J.: Fortran IV Computer Program for Calculating Critical Speeds of Rotating Shafts. NASA TND-7385, 1973.
35. Jones, A. B.; and McGrew, Jr., J. M.: "Rotor-Bearing Dynamics Technology Design Guide." AFAPL-TR-78-6, Air Force Aero Propulsion Lab.; Pt. 2-Ball Bearing, 1978 (AD-A065554); Pt. 4-Cylindrical Roller Bearings, 1979 (AD-A082355).
36. Nestorides, E. J.: A Handbook on Torsional Vibration. Cambridge Univer. Press, 1958.
37. Thomson, W. T.: Theory of Vibration with Applications. Second ed., Prentice-Hall, 1981.

1. Report No. NASA RP-1123		2. Government Accession No.		3. Recipient's Catalog No.	
4. Title and Subtitle Design of Power-Transmitting Shafts				5. Report Date July 1984	
				6. Performing Organization Code 505-40-42	
7. Author(s) Stuart H. Loewenthal				8. Performing Organization Report No. E-1899	
				10. Work Unit No.	
9. Performing Organization Name and Address National Aeronautics and Space Administration Lewis Research Center Cleveland, Ohio 44135				11. Contract or Grant No.	
				13. Type of Report and Period Covered Reference Publication	
12. Sponsoring Agency Name and Address National Aeronautics and Space Administration Washington, D.C. 20546				14. Sponsoring Agency Code	
15. Supplementary Notes Published as part of Chapter 34 in Mechanical Design and Systems Handbook, H. A. Rothbart, ed., Second edition, McGraw-Hill Book Co., 1984.					
16. Abstract Power transmission shafting is a vital element of all rotating machinery. This report summarizes design methods, based on strength considerations, for sizing shafts and axles to withstand both steady and fluctuating loads. The effects of combined bending, torsional, and axial loads are considered along with many application factors that are known to influence the fatigue strength of shafting materials. Methods are presented to account for variable-amplitude loading histories and their influence on limited-life designs. The influences of shaft rigidity, materials, and vibration on the design are also discussed.					
17. Key Words (Suggested by Author(s)) Shaft Fatigue Shafting Design			18. Distribution Statement Unclassified - unlimited STAR Category 37		
19. Security Classif. (of this report) Unclassified		20. Security Classif. (of this page) Unclassified		21. No. of pages 23	22. Price* A02